



Research Article

Enhancement of 5-Hydroxymethylfurfural and 2,5-Furandicarboxylic Acid Extractions into Bio-Plastic Production from Renewable Sources

Payam Ghorbannezhad ^{a,b*}, Behnam Dehbandi ^c, Imtiaz Ali ^d

^a Department of Biorefinery, Faculty of New Technologies Engineering, Shahid Beheshti University, Tehran, Iran.

^b Alliance for Biomass and Sustainability Research-ABISURE, National University of Colombia, Campus Robledo, M3-214, Medellín, Colombia.

^c Department of Chemistry, Science and Research Branch, Islamic Azad University, Tehran, Iran.

^d Department of Chemical and Materials Engineering, King Abudlaziz University, Rabigh, Suadia Arabia.

PAPER INFO

Paper History:

Received: 28 July 2022

Revised: 08 October 2022

Accepted: 21 October 2022

Keywords:

5-Hydroxymethylfurfural (HMF),
2,5-Furandicarboxylic Acid (FDCA),
Renewable Sources,
Density Function Theory (DFT)

A B S T R A C T

Furandicarboxylic acid (FDCA) is recognized as a valuable product of hydroxymethylfurfural (HMF) derived from cellulosic materials as an abundant renewable source. It could find future bioplastic application if a feasible separation process is developed. To find a commercially available solvent, FDCA should be selectively separated from HMF and the downstream process be supported by pyrolysis-gas chromatography-mass spectrometry experiments in line with density functional theory (DFT). Evaluation of the sigma potential and sigma surface analysis demonstrated that benzene and ethyl acetate enjoyed better extraction and HMF selectivity, whereas FDCA exhibited ideal behavior in the presence of DMF and DMSO solvents. It was proved that the hydrophobicity could be changed by improving the hydrogen-bonding interaction between them. Moreover, the up-down selection of classes of solvents based on the experimental data found by GC-MS revealed that polar molecular solvents (ethanol-water) were more compatible with carboxylic acids and alcohol compounds, while n-hexane was a desirable solvent for phenolic compounds. It was found that levoglucosan retained a significant fraction of water compared to other solvents, which need to be considered for further economic and environmental analysis under the multifaceted framework of biomass-derived products.

<https://doi.org/10.30501/jree.2022.353576.1415>

1. INTRODUCTION

Recently, bioplastics have become promising feedstocks for value-added products that have the potential to replace fossil fuel-based petrochemicals. Petrochemicals pose environmental and climate-related challenges to our society. Environmental concerns increase when chemical manufacturers expand their product portfolio and increase production due to the continuously increasing demand for polymeric materials. More than 8000 Mt of plastics continue to be consumed annually, roughly 80 % of which have ended up in landfills and oceans (Geyer et al., 2017). This is because as consumers, we are becoming more addicted to single-use disposable plastics. Based on the prediction made by the U.S. Department of Energy (DOE), plastic manufacturers will consume 20 % of all petroleum materials with a share of 15 % annual global carbon emissions by the year 2050 (Perlack et al., 2011). The global warning that arises from plastic production, consumption, and waste management requires

renewable chemical strategies (Erickson & Winters, 2012; Zheng & Suh, 2019).

Biorefinery is recognized as a valuable route to biomass as a feedstock that can reduce our dependence on fossil fuels (Stuart & El-Halwagi, 2012). Biomass is an abundant feedstock with great potential to produce biofuels, biochemical, and bioproducts (Bilal et al., 2021; Ghorbannezhad et al., 2020). Today, more than 100 billion tons of biomass is available around the world, most of which end up as waste due to ineffective technologies (Dutta et al., 2014; Searle & Malins, 2015). Biomass can completely boost bioeconomy by rebuilding fuel and chemical manufacturing processes.

Lignocellulosic biomass is made up of carbohydrate polymers, such as cellulose (40-50 %) and hemicellulose (20-40 %), and aromatic polymers, such as lignin (20-30 %). These chemical components are the main building blocks of many biochemical platforms (Figure 1).

5-hydroxymethylfurfural (HMF) is recognized as a high-value building block compound of cellulose that can be transformed into a variety of value-added chemicals (Davidson et al., 2021; Kuster, 1990; Rosatella et al., 2011). HMF is recognized as the "top 10" chemical platform in the

*Corresponding Author's Email: p_ghorbannezhad@sbu.ac.ir (P.

Ghorbannezhad)

URL: https://www.jree.ir/article_160756.html



circular bioeconomy by DOE. It is synthesized by the dehydration of mono and polysaccharides present in lignocellulosic biomass. Furanicarboxylic acid (FDCA) is one of the most valuable biochemicals that can be derived from HMF via biological or chemical oxidation (Arikan et al., 2021). During conversion, the oxidation of the aldehyde of

HMF produces 5-hydroxymethyl-2-furan carboxylic acid, which is an intermediate compound. Further oxidation of 5-hydroxymethyl-2-furan carboxylic acid produces furan carboxylic acid (FFCA), which finally turns into FDCA. The schematic of cellulose conversion is shown in Figure 2.

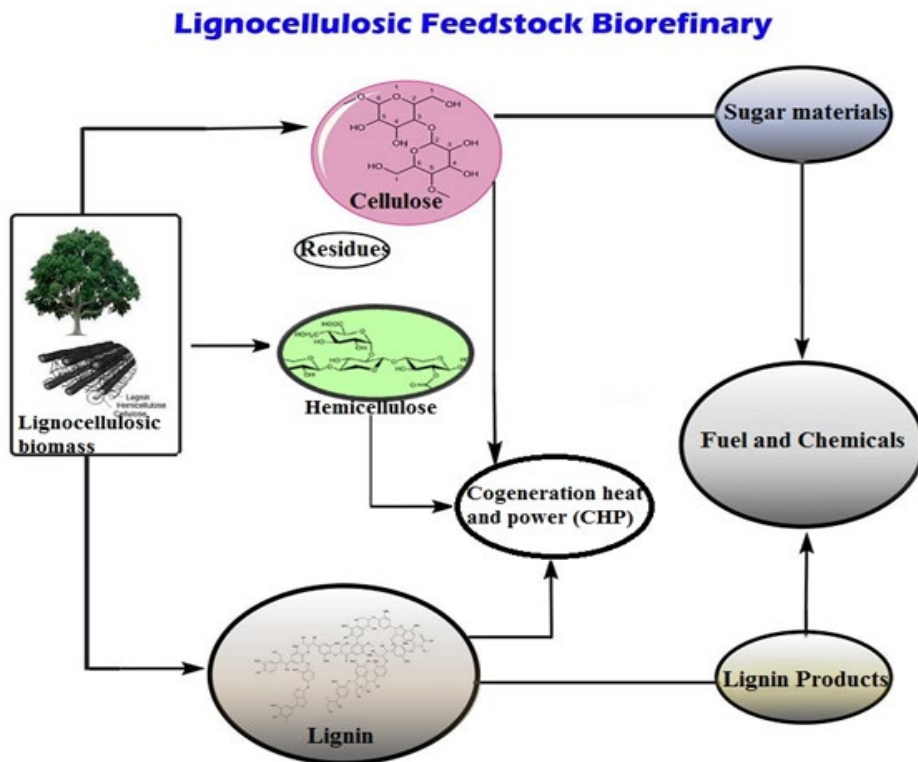


Figure 1. Pathways of value-added products from lignocellulosic components

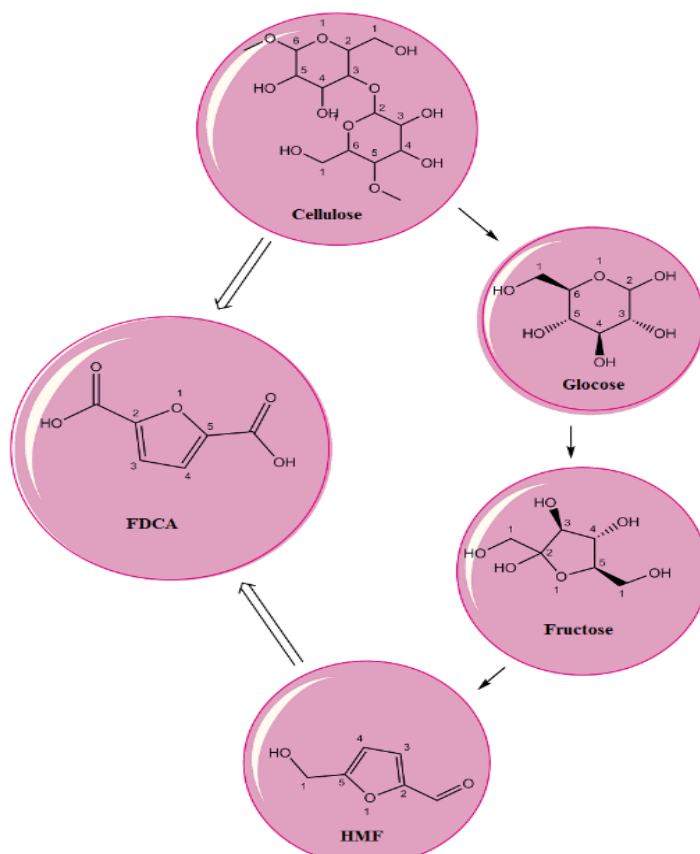


Figure 2. Overview of FDCA production pathways from cellulose

Therefore, one of the most cost-effective FDCA production routes is the direct conversion of biomass into desired products on a commercial scale (Arikan et al., 2021; Hwang et al., 2020). In this regard, condensation reactions under acidic aqueous conditions must be suppressed by substituting an organic solvent during the rehydration process (Bonner et al., 1960). Solvents are vital to obtain a higher yield of HMF and its derivatives. Currently, direct dehydration of glucose to produce HMF and its derivatives is limited by an inefficient separation process (Bello Ould-Amer et al., 2020; Cai et al., 2013; Hou et al., 2017; Motagamwala et al., 2019; Zunita et al., 2021). FDCA exhibits low solubility in water and the problem of deactivation during the direct conversion of glucose into HMF in water as a solvent (Esteban et al., 2020; Zhang et al., 2018). The weak separation efficiency for short-chain solvents led to high volumetric consumption of organic solvents and salts to make a biphasic system. However, selecting an efficient solvent for purification and separation of products is a new research area to develop biorefinery processes. Methyl isobutyl ketone (MIBK), tetrahydrofuran (THF), and dimethyl sulfoxide (DMSO) have been used as moderately polar and highly dielectric solvents to promote the dehydration reaction for HMF production (Weingarten et al., 2014). The authors have indicated that the solvents increased the dehydration reaction, but reduced the polymerization of HMF. Some studies revealed that biphasic system aims to improve the HMF yield via in situ extraction of HMF at the organic phase. A higher partition coefficient of HMF can lead to increased productivity and make the process cost-effective (Blumenthal et al., 2016). The computational method applies a heuristic approach that estimates the activity coefficient to identify appropriate solvents. The combination of quantum mechanics and statistical mechanics presents multifunctional models to better describe molecular thermodynamics. Unlike empirical models such as UNIFAC, ASOG, etc., the conductor-like screening model for real solvents (COSMO-RS) can explain intermolecular interactions (Balchandani & Singh, 2021; Klamt, 2018). An ensemble of pairwise intermolecular interactions in COSMO-RS provides a significant deviation in phase behavior, leading to crucial insights on different solvent classes (Eckert & Klamt, 2018). Density Function Theory (DFT) can be combined with COSMO-RS to optimize the performance of models (Momany & Schnupf, 2014; Wang et al., 2020). This work aims to investigate and predict the thermodynamic properties of cellulose derivatives obtained from biomass. Five samples including HMF, DFF, HMFCA, FDCA, and FFCA were studied. Flash points, boiling points, Henry's constant, activity coefficients, Vapor-Liquid Equilibrium (VLE), and Liquid-Liquid Equilibrium (LLE) were obtained for various solvents and different dielectric constants. The products were identified and predicted via thermodynamic properties that have not been reported before.

2. MATERIALS AND METHODS

2.1. Pyrolysis tandem microreactor

The experimental pyrolysis of biomass was performed in Rx-300 TR, a tandem micropyrolyzer system from Frontier Laboratories, Japan. The system is classified into two parts: a) pyrolysis reactor with a steady amount of biomass of 1-2 mg and b) catalyst bed reactor. Hence, you do not use the catalysts; you can set the reactor temperature to the same value as the pyrolysis reactor temperature. About 2 g of the

milled biomass samples were placed in a stainless steel cup to drop into the first reactor. Helium as a neutral carrier gas (1 ml/min) transfers the vaporized biomass compound from the thermal degradation reactor to the catalyst bed reactor. A temperature of 500 °C with a heating rate of 10 °C.min⁻¹ is fitted by a programmable temperature control to maintain a constant process condition. The hot vapor (syngas) is retained in the first reactor for less than 2 seconds and, then, goes into the catalyst bed reactor, which is finally detected by GC-MS interfaced with the pyrolysis system. The percentage area peak of each compound could be determined to estimate the yield of products individually.

2.2. Computational methods and theory

COSMO-RS is the conductor-like screening model for real solvation that uses Quantum Chemistry (QC) to predict the thermodynamic properties of molecules (Klamt., 1995; Klamt., 2005). The molecules are embedded in a virtual conductor based on the polarization charge densities of the solute and solvent molecules. DFT can be combined with the COSMO as it is available in most quantum chemical programs. The structure of the biomass used in this study was drawn manually using the Gauss view software, which was further optimized with the Gaussian 09 program (Forlemu et al., 2017). From the optimized structure, COSMO, sigma profile potential, and frequency files were generated. With the level of theory, Becke's three-parameter functional for exchange was combined with the nonlocal correlation potential of the Lee-Yang-Parr functional and the DGTZVP basis set (Godbout et al., 1992; Klamt et al., 2016). One of the important COSMO-RS calculations is to estimate the sigma profile of each sample studied. The specific interactions of each of the molecules at the aqueous phase were defined in COSMO-RS. The quantum mechanical characterization of solvents, such as electrostatic interactions and hydrogen bonding as well as local interactions of surface segments, was calculated and screened by the charge density profile σ and stored in the COSMO-RS database. The segment interaction of individual solvents determined the efficiency and solubility of the compositions via statistical thermodynamic calculations for the interacting surfaces. The free energies and chemical potentials of the molecules in pure and mixed solvents result from the efficiency of solubility and separation for each composition. In this work, the COSMO-RS calculations were performed using the COSMOtherm (Cosmologic GmbH, Leverkusen, Germany) program with BP_TZVPD_18 (Zhao et al., 2020). The geometries and conformations used for the solutes and solvents were generated and handled in the COSMO-RS calculations, as described before (Eckert & Klamt, 2018). By using the COSMOtherm program, the thermodynamic properties of the extracted chemical compounds can be predicted, such as flashpoints, boiling point, density, activity coefficient, σ surface, σ potential, Liquid Vapor Equilibrium (VLE), Liquid-Liquid Equilibrium (LLE), vapor pressure, Henry's law coefficient, and hexane-water partition coefficients at different solvents, temperatures, and pressures. In COSMO, the σ profile of molecule X (Equation 1) and the chemical potential of a surface segment with screening charge density (Equation 2) were obtained. Each molecule X is described by its surface composition histogram with respect to σ , the so-called σ -profile $p_X(\sigma)$, and a pure or mixed liquid system is characterized by its solvent σ -profile.

$$p^{x_i}(\sigma) = \frac{n_i(\sigma)}{n_i} = \frac{A_i(\sigma)}{A_i} \quad (1)$$

where $A_i(\sigma)$ is the segment surface area that has charge density σ , x_i the mole fraction of the i th molecule x , A_i the area of the whole surface cavity rooted in the medium.

$$\mu_s(\sigma) = -\frac{RT}{a_{\text{eff}}} \ln \left[\int p_s(\sigma') \exp \left\{ \frac{a_{\text{eff}}}{RT} [\mu_s(\sigma') - e(\sigma, \sigma')] \right\} d\sigma' \right] \quad (2)$$

where $\mu_s(\sigma')$ is the chemical potential of a surface segment. $\mu_s(\sigma)$ expresses the attraction of a solvent S to surface segments of polarity σ . σ is the polarity of the surface under study.

Table 1. Properties, energy efficacy, and toxicity of the studied solvents (Zhao et al., 2020)

Solvents	Properties				Energy efficiency			
	Molecular weight (g/mol)	Viscosity (mPa/s)	Log P	Flash point (°C)	Boiling point (°C)	ΔH vap. (kJ/mol)	Cp liq. (J.kg ⁻¹ K ⁻¹)	Energy evaporation (kJ/mol)
Water	18.01	1.0016	-0.65	N/A	100	40.65	4185.5	40.6
Ethanol	46.07	0.983	-0.24	12	78	38.56	2.57	38.5
Methanol	32.04	0.543	-0.76	11	65	35.21	2.53	35.2
DMSO	78.13	2	-1.37	88.88	189	52.9	149.40	52,5
DMF	73.09	0.92	-1	60	153	56.7	146.05	46.7
Benzene	78.11	0.603	2	-11	80	30.72	133	33.8
Ethyl-Acetate	88.11	0.426	0.71	-4.44	77	31.94	161.47	31,9
CCl ₄	153.82	0.965	2.8	982	77	29.82	133.0	30
Hexane	86.18	0.3	3.764	-7	69	28.85	265.2	28.8

3. RESULTS AND DISCUSSION

3.1. Sigma potential analysis

The δ -potential describes the possible interaction of compounds with solvents according to polarity and hydrogen bonding. Molecular interactions between the solvents and HMF play a vital role in HMF solubility. The shape, size, and initial components of the molecule are essential for molecular interaction. Caloric profiles provide important information to predict molecular interactions at the fluid phase. The hydrogen bond acceptor, hydrogen bond donor, and non-polar area associated with red, blue, and green, respectively, are shown in Figure 3. For δ -surface, the negative screening charge density represented the positive polarity. In general, acceptor hydrogen bonds have a negative charge density, whereas the donor hydrogen shows a positive charge density. For example, there are negative and positive sides to n-hexane. The negative side corresponds to hydrogens, whereas the positive side corresponds to carbons. In general, n-hexane shows a polar alkane characterization when the δ -potential is near zero.

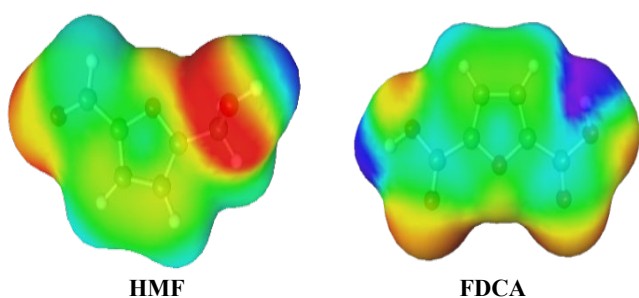


Figure 3. Sigma surface of HMF, HFDCA, FFCA, and FDCA

3.2. Chemical compositions of solvents

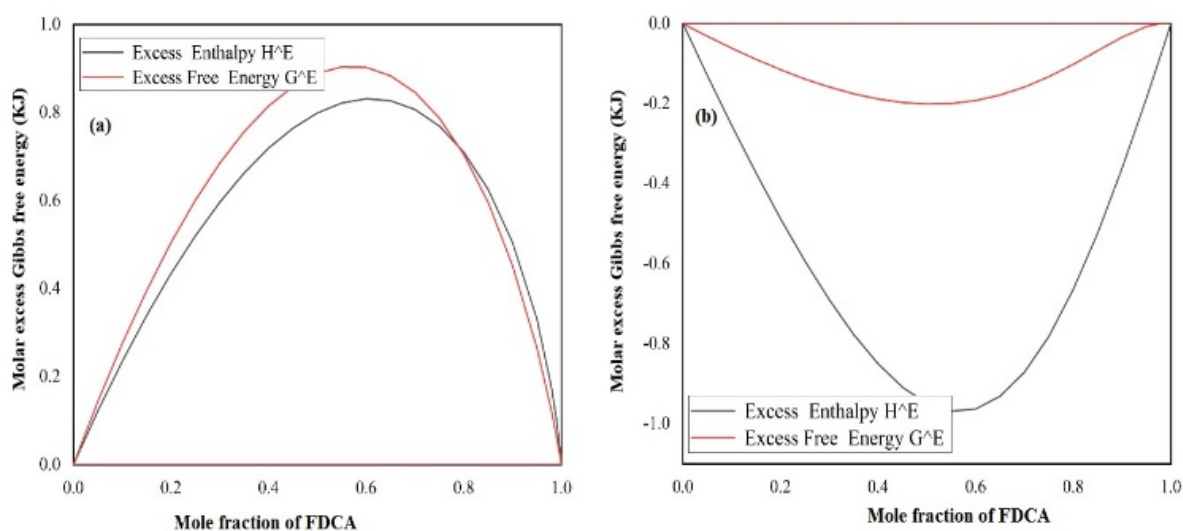
Several chemical compositions were obtained by GC-MS of biomass. The concentrated aqueous solution of cellulose enhances the generation of HMF. Water as a solvent resulted in higher HMF and levulinic acid converted into 2-MTHMF, butanols, and acid. Table 2 shows the chemical composition of cellulose in different solvents identified by GC-MS. The results showed that the DMF exhibited lower performance than ethyl acetate and hexane in water. More acid and esters (aliphatic compounds) were separated by ethanol-water solvents, whereas more aromatic compounds could be extracted by hexane and benzene as solvents. It is assumed that the low solubility of hydrocarbons in water results from the reduction of the polarity differences. Typically, polar solvents enhance HMF and carboxylic acid extraction by 20 %. Cellulose is anticipated to reduce the solubility of phenolic compounds in water and affect the overall separation process.

3.3. Excess energies of FDCA and HMF solvents

The free energy derivative validated the simulation of the interaction of FDCA separation in water and n-hexane, which corresponded to the process. The interaction of FDCA separation in n-hexane showed a Gibbs free energy value of + 0.8 kcal.mol⁻¹, whereas the same purification process in water is - 0.9 kcal.mol⁻¹ (Figure 4). However, n-hexane can be placed in the middle of the solvents, which could theoretically dissolve all compounds equally. Gibbs free energy is positive for n-hexane, illustrating low solubility limits for all concentration levels. The solubility of water at the organic phase of FDCA is lower than that of n-hexane. Thus, the Gibbs free energy presents a highly negative area in water.

Table 2. Chemical compositions of solvent extraction by GC-MS

Compounds	Water	Ethanol	Methanol	DMSO	DMF	Benzene	Ethyl acetate	CCl ₄	Hexane
Acids									
Acetic acid	2.6	2.7	2.1	1.9	1.2	1.6	1.5	1.6	1.5
Formic acid	0.8	0.9	0.4	0.4	0.5	0.5	0.5	0.6	0.5
Propionic acid	0.8	1.1	0.5	0.7	0.6	0.7	0.7	0.8	0.6
Hexadecanoic acid	0.5	0.7	0.4	0.3	0.1	0.3	0.2	0.2	0.3
Benzeoic acid	0.4	0.7	0	0.4	0.2	0.4	0.3	0.4	0.4
Levulinic acid	1.2	1.7	1.4	0.9	0.9	0.9	1.1	1.1	0.8
Ketones									
1-Hydroxy-2-propanone	1.6	1.6	1.2	1.3	1.4	1.4	1.4	1.4	1.4
Butanone	0.5	0.7	0.3	0.2	0.2	0.2	0.2	0.2	0.2
1,2-Cyclopentanedione	1.1	1.5	1.2	1.1	0.9	0.9	1.2	0.8	0.6
3-Methyl-1,2-cyclopentadione	0.7	1.1	1.6	0.7	0.6	0.7	0.5	0.5	0.6
Furanones	0.9	1.2	0.7	0.2	0	0.2	0.2	0.3	0.2
Furans									
Furfural	0.6	0.5	0.6	1.7	1.8	1.7	1.7	0.9	1
Hydroxymethylfurfural	0.4	0.6	0.6	1.5	1.5	1.9	1.8	1.3	1.1
Methylfurfural	0.2	0.3	0	1.1	1.2	0.8	0.9	0.2	0
Phenols									
Ethyl-Phenol	0.5	0.4	0.4	0.4	0.4	0.3	0.3	0.3	2.3
Phenol	1.4	1.8	2.1	2.1	2.25	2.1	1.1	1.5	4.5
Guaicols	1.9	1.1	1.02	1.4	1.5	1.4	1.2	1.15	3.35
Cresol	0	0.3	0.1	0.3	0.2	0.5	0.1	0.3	2.1
Methoxyphenols	0.4	0.5	0.3	0.5	0.3	0.4	0.3	0.3	2.3
Vaniline	0	0.4	0	0.4	0.3	0.4	0.3	0.3	0.7
Anhydro sugars									
Levoglocosan	10.1	9.3	6.7	6.35	6.85	4.75	7.1	4.1	4.1
1,6-Anhydro-a-d-galactofuranose	4.6	5.1	3.1	3.5	3.6	3.5	4.2	3.8	2.1
Cellobiosan	1.1	1.9	1.3	0.8	0.9	1.2	1.2	1.2	0.8

**Figure 4.** Gibbs tangent plane diagram for FDCA solvents (a: n-hexane; b: water)

On the other hand, Gibbs energy of mixing is positive for an HMF-water system for the entire concentration range due to its very low mutual solubility limits. Given that HMF-water is partially miscible, the solubility of water at the organic phase is higher than the aqueous solubility. Thus, the Excess Enthalpy of the mixing plot shows the negative region in the HMF region, as shown in Figure 5. The HMF-water shows a maximum miscibility gap of a mole fraction of 0.9. Moreover,

the Gibbs energy and excess enthalpy of mixing are negative for an FDCA-water system in the entire concentration range due to its mutual solubility limits. FDCA-water is partially miscible and the solubility of water at the organic phase is higher than the aqueous solubility. Therefore, the Gibbs energy and excess enthalpy of the mixing plot show the negative region in the middle of the FDCA-water region, as shown in Figure 4 (b).

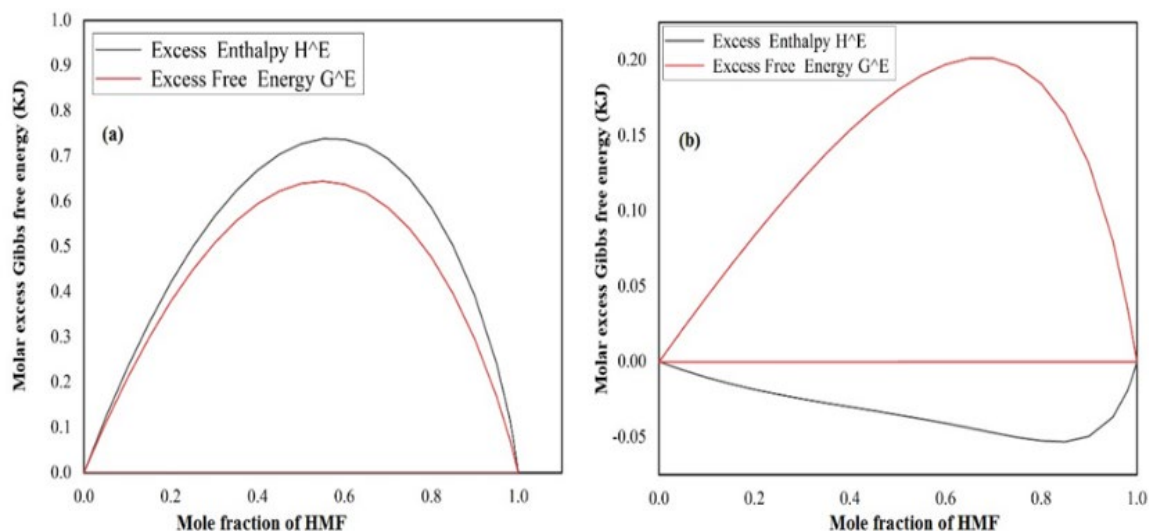


Figure 5. Gibb's tangent plane diagram for the HMF solvents (a: n-hexane; b: water)

The excess energies (G_{ex} and H_{ex}) for HMF at solvents of water, hexane at 298.15 K is shown Figure 5. The G_{ex} energy of HMF mixture with water indicated the positive value of ~ 0.2 kJ/mol at $x_1 = 0.7$ while H_{ex} energy of HMF mixture with water is with a minimum of -0.05 kJ/mol at $x_1 = 0.8$. The HMF mixture with hexane showed a value G_{ex} energy of ~ 0.6 kJ/mol at $x_1 = 0.6$ and the H_{ex} with a minimum of 0.7 kJ/mol at $x_1 = 0.65$. In the present work, we investigate the solvents system and mole fraction solvents for the solubility of a solid solute in the liquid mixture using COSMO-RS and COSMO SAC methods. Optimized maximum solubility using COSMO-RS and COSMO SAC methods revealed that DMSO solvent was the best solvent for Hydroxymethylfurfural solubility. The value of HMF mole fraction was obtained $X = 0.707986$ and for DMSO $X = 0.29201$ through COSMO-RS method and also via COSMO SAC methods. The mole fraction values of 0.656330 , 0.34367 were calculated for HMF and DMSO, respectively. Therefore, DMSO is selected as the best solvent for solubility 2, 5-Furandicarboxylic. In this regards, mole fraction value of FDCA were $X = 0.372261$, DMSO $x = 0.29201$ via the COSMO SAC methods while the mole fraction value of FDCA was 0.156783 , and a DMSO is 0.84322 via COSMO-RS method.

3.4. Activity coefficients and validation

To calculate activity coefficients on the mole fraction scale for each solute (HMF/FDCA) in an infinite dilution state using COSMO-RS and COSMO SAC methods, the mole fraction of

the solute is set to zero in the composition of the solution and the reference state is the pure solute. CosmoTherm calculates the natural logarithmic value of the activity coefficient using the pseudo-chemical potentials of the compound both in its pure and fully dissolved forms in a solvent. It can be observed that the activity coefficient for the components HMF and FDCA is quite high in case of infinite dilution at hexane higher than water. This means that the activity coefficients and intermolecular interactions of different solutes in solvents are quite dependent on the chemical structure of solute HMF and FDCA.

This non-ideality is attributed to the degree of dissociation/reaction of the solute in the solute-solvent interactions such as complex ion formation and in the solute-solute interactions such as ion pairing. An activity coefficient incorporates particle interactions into a single term so that the formal concentration can be modified to give an estimate of the effective concentration, or activity, of each ion. The partition coefficients ($\log P$) of infinitely diluted solutes in a mixture of two immiscible solvents can be calculated with Partition Coefficients ($\log P$). They were used for calculating ethanol/water, benzene/water, ether/water, and hexane/water partition coefficients (Table 3). In the case of partly miscible liquids, like the ethanol-rich phase of ethanol and water, both components have nonzero mole fractions. The following table presents the value of the molar volume quotient of the two solvents.

Table 3. The partition coefficient (LOG P) of mixture solvents

Compound	Ethanol/Water	Benzene/Water	Hexane/Water	Ether/Water
HMF	-0.8337	-1.9507	-3.5269	0.1151
FDCA	0.4527	-3.4778	-5.1710	2.9823

3.5. COSMO-RS prediction optimized by DFT

The sigma potential determines the pseudochemical potential of the molecular surface. The chemical potential of the surface segment was obtained by thermodynamics of molecular interactions. Using COSMO-RS theory, one can calculate the thermodynamic properties of fluids from the 3D polarized charge distribution of individual molecules (σ -surface) in

terms of σ -profile (2D histogram). Thus, valuable information regarding the polarity of a compound and its interaction with other surrounding molecules in the fluid media can be deduced from these σ -profile histograms. Figure 6 shows PX (σ), the charge density of these compounds in the polarized field (σ). The following criteria can be applied to divide the field into three regions: $\sigma > +0.0082$ e/Å⁻² as the hydrogen bond (HB) acceptor region; the hydrogen bond (HB) donor

region having $\sigma < -0.0082 \text{ e}/\text{\AA}^2$; and the nonpolar region between $-0.0082 < \sigma < +0.0082 \text{ e}/\text{\AA}^2$. The sigma profile of ethanol and methanol exhibited a positive potential for the polar surface segment ($\delta > 0.05 \text{ e}/\text{\AA}^2$), implying unfavorable solvation for HMF extraction. It is manifested that ethanol and methanol are miscible with water. It is revealed that the HMF is a strong hydrogen bond donor because of the higher profile area which facilitates water interaction. In order to evaluate the validation of Cosmo-RS models, the experimental data of mixture solvents is performed. The experimental attempts on

mixture solvents validated these predictions at room temperature. σ -potential of thanol/water is similar to benzen/water for extraction of HMF while DMF solvent nearly is immiscible in water. It is revealed that the hydroxymethyl group of HMF is a hydrogen-bonding donor from aqueous media. On the contrary, benzene and ethyl acetate solvents show a descending sigma potential sinking below $-0.15 \text{ kcal}\cdot\text{mol}^{-1}\cdot\text{\AA}^{-2}$ for the surface charge density at $0.05 \text{ e}/\text{\AA}^2$, where efficient HMF separation takes place (Figure 6).

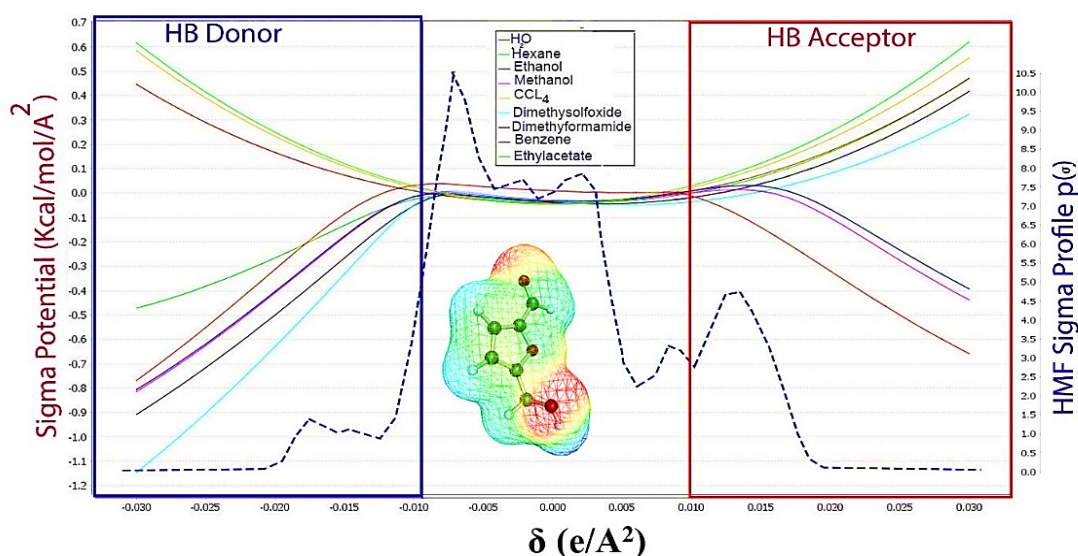


Figure 6. δ -potential & profile of HMF (dotted line) with solvents (solid lines)

The sigma potential profiles suggest DMF and DMSO as the alternative and most promising solvents for FDCA extraction. The hydrophobicity region at $\delta = 0$ reflected the potential difference in the solubility of the solvents with water. Benzene and ethyl acetate enable direct bonding to the OH group, resulting in increase in the nonpolar alkyl group and the rise of the hydrophobicity. On the other hand, DMF and DMSO replace the hydrophilic environment to improve the selectivity and overall yield of FCDA (Figure 7). In fact, the low mutual solubility of DMF and DMSO makes them not eligible to interact on hydrogen bonding. Thus, DMF and DMSO

exhibited a lower charge density in hydrogen bonding, which results in less interaction with water and better fractionation of the organic phase. Thus, nonpolar organic and hydrocarbon compounds with π - π bond are more favorable with DMF and DMSO solvents because of fewer interactions with the hydrogen bond. Nevertheless, it is interesting to note that there are clear differences in the interactions of solvents with HMF and FDCA. In FDCA, these peaks were found at higher positive polarity, showing a stronger HB acceptor character of the carboxylate group rather than the hydroxyl methyl group in the homologous HMF.

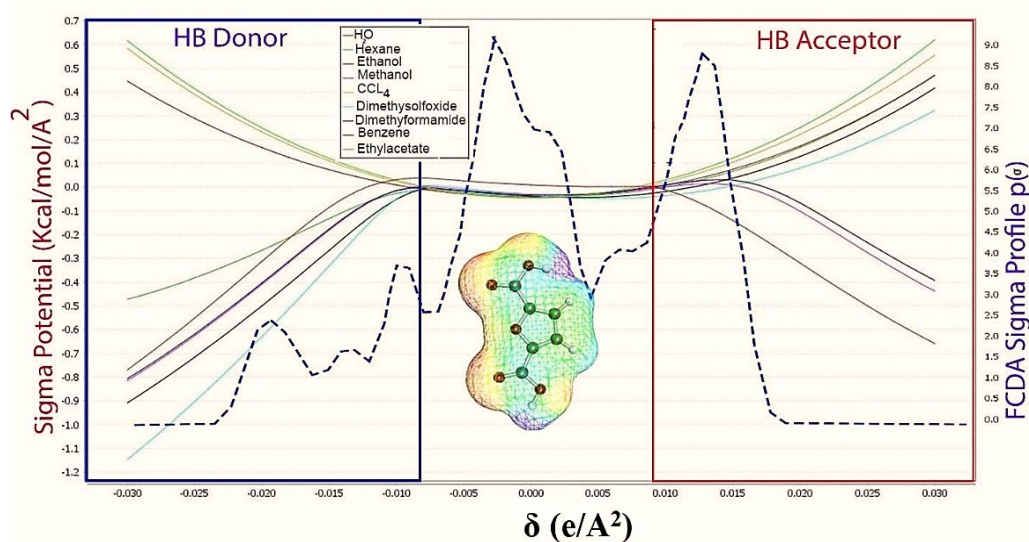


Figure 7. δ -potential & profile of FDCA with solvents

Thus, different profiles of σ -surface are contributed independently of each atom related to its charge density as well as the descriptor of each constituent in the solvents. Finally, with stronger HB donor and HB acceptor groups, COSMO-RS describes FDCA as a more polar structure than those of the homolog HMF. Consequently, the results of this study aimed to develop a framework of models that could predict the quantum-chemical properties of solvents to screen the interactions between them. It is purely a prediction approach to COSMO-RS optimized by the DFT methodology. On the other hand, it provides an efficient final product that is rich in HMF and FDCA and approves the emerging biobased molecules for commercializing green processes. Therefore, the efficient solvent design approach would be highly reliable based on experimental data in the applicability domain for green and sustainable bioplastic manufacturing processes.

4. CONCLUSIONS

This study aims to evaluate the efficiency of different solvents for the desirable extraction of HMF and FDCA for future bioplastic industries. A multiscale COSMO-RS model on a desirable solvent system was optimized by DFT methodology. Evaluation of the sigma potential and sigma surface analysis showed that benzene and ethyl acetate had better extraction and selectivity toward HMF. Moreover, FDCA exhibited ideal behavior in DMF and DMSO solvents. GC-MS data revealed that the polar molecular solvent (ethanol-water) extracted more carboxylic acids and alcohols, while n-hexane lied in the middle of the solvents for phenolic compounds. Experimental data confirmed that HMF was more convenient by polar molecular solvents that were miscible in water while the FDCA extraction solvents were immiscible in water. It is worth noting that the higher aromatics in HMF promote the Diels-Alder reaction as well as the dehydration reaction. Thus, a promising route for the generation of FDCA from HMF could be through the use of strong concentrations of cellulose. In addition, DMF and DMSO improved the hydrogen bonding interaction between FDCA and solvent molecules and, thus, led to efficient separation. However, the strategy employed in this study could be considered as a computational prediction to select a favorable solvent with efficient bioplastic manufacturing processes.

5. ACKNOWLEDGEMENT

This study was supported partially by department of biorefinery engineering at Shahid Beheshti University, Iran (award number: 397081). The authors also want to thank the Alliance for Biomass and Sustainability Research-ABISURE "Universidad Nacional de Colombia" Hermes code 5302, for the partial support to this work.

REFERENCES

1. Arıkan, E.B., Bouchareb, E.M., Bouchareb, R., Yağcı, N., & Dizge, N. (2021). Innovative technologies adopted for the production of bioplastics at industrial level. In: Kuddus, M., Roohi (eds), *Bioplastics for Sustainable Development* (pp. 83-102), Springer, Singapore. https://doi.org/10.1007/978-981-16-1823-9_3
2. Balchandani, S., & Singh, R. (2021). Thermodynamic analysis using COSMO-RS studies of reversible ionic liquid 3-aminopropyl triethoxysilane blended with amine activators for CO₂ absorption. *Journal of Molecular Liquids*, 324, 114713. <https://doi.org/10.1016/j.molliq.2020.114713>
3. Bello Ould-Amer, S., Méndez Trelles, P., Rodil Rodríguez, E., Feijoo Costa, G., & Moreira Vilar, M.T. (2020). Towards improving the

sustainability of bioplastics: Process modelling and life cycle assessment of two separation routes for 2, 5-furandicarboxylic acid. *Separation and Purification Technology*, 233, 116056. <https://doi.org/10.1016/j.seppur.2019.116056>

4. Bilal, M., Vilar, D.S., Eguiluz, K.I.B., Ferreira, L.F.R., Bhatt, P., & Iqbal, H.M.N. (2021). Biochemical conversion of lignocellulosic waste into renewable energy. In *Advanced Technology for the Conversion of Waste into Fuels and Chemicals* (pp. 147-171), Elsevier. <https://doi.org/10.1016/B978-0-12-823139-5.00007-1>
5. Blumenthal, L.C., Jens, C.M., Ulbrich, J., Schwering, F., Langrehr, V., Turek, T., Kunz, U., Leonhard, K., & Palkovits, R. (2016). Systematic identification of solvents optimal for the extraction of 5-hydroxymethylfurfural from aqueous reactive solutions. *ACS Sustainable Chemistry & Engineering*, 4(1), 228-235. <https://doi.org/10.1021/acssuschemeng.5b01036>
6. Bonner, T.G., Bourne, E.J., & Ruszkiewicz, M. (1960). The iodine-catalysed conversion of sucrose into 5-hydroxy-methylfurfuraldehyde. *Journal of the Chemical Society (Resumed)*, 787-791. <https://doi.org/10.1039/JR9600000787>
7. Cai, C.M., Zhang, T., Kumar, R., & Wyman, C.E. (2013). THF co-solvent enhances hydrocarbon fuel precursor yields from lignocellulosic biomass. *Green Chemistry*, 15(11), 3140-3145. <https://doi.org/10.1039/C3GC41214H>
8. Davidson, M.G., Elgie, S., Parsons, S., & Young, T.J. (2021). Production of HMF, FDCA and their derived products: A review of life cycle assessment (LCA) and techno-economic analysis (TEA) studies. *Green Chemistry*, 23, 3154-3171. <https://doi.org/10.1039/D1GC00721A>
9. Dutta, S., Bhaumik, A., & Wu, K.C.-W. (2014). Hierarchically porous carbon derived from polymers and biomass: effect of interconnected pores on energy applications. *Energy & Environmental Science*, 7(11), 3574-3592. <https://doi.org/10.1039/C4EE01075B>
10. Eckert, F., & Klamt, A. (2018). *COSMOtherm*, version 18.0.0. COSMOlogic GmbH & CoKG: Leverkusen, Germany.
11. Erickson, B., & Winters, P. (2012). Perspective on opportunities in industrial biotechnology in renewable chemicals. *Biotechnology Journal*, 7(2), 176-185. <https://doi.org/10.1002/biot.201100069>
12. Esteban, J., Vorholt, A.J., & Leitner, W. (2020). An overview of the biphasic dehydration of sugars to 5-hydroxymethylfurfural and furfural: A rational selection of solvents using COSMO-RS and selection guides. *Green Chemistry*, 22(7), 2097-2128. <https://doi.org/10.1039/C9GC04208C>
13. Forlemu, N., Watkins, P., & Sloop, J. (2017). Molecular docking of selective binding affinity of sulfonamide derivatives as potential antimalarial agents targeting the glycolytic enzymes: GAPDH, Aldolase and TPI. *Open Journal of Biophysics*, 7, 41-57. <http://dx.doi.org/10.4236/ojbiphy.2017.71004>
14. Geyer, R., Jambeck, J.R., & Law, K. L. (2017). Production, use, and fate of all plastics ever made. *Science Advances*, 3(7), e1700782-e1700782. <https://doi.org/10.1126/sciadv.1700782>
15. Ghorbannezhad, P., Park, S., & Onwudili, J.A. (2020). Co-pyrolysis of biomass and plastic waste over zeolite- and sodium-based catalysts for enhanced yields of hydrocarbon products. *Waste Management*, 102(December), 909-918. <https://doi.org/10.1016/j.wasman.2019.12.006>
16. Godbout, N., Salahub, D.R., Andzelm, J., Wimmer, E. (1992). Optimization of Gaussian-type basis sets for local spin density functional calculations. Part I. Boron through neon, optimization technique and validation. *Canadian Journal of Chemistry*, 70, 560-571. <https://doi.org/10.1139/v92-079>
17. Hou, Q., Li, W., Zhen, M., Liu, L., Chen, Y., Yang, Q., Huang, F., Zhang, S., & Ju, M. (2017). An ionic liquid-organic solvent biphasic system for efficient production of 5-hydroxymethylfurfural from carbohydrates at high concentrations. *RSC Advances*, 7(75), 47288-47296. <https://doi.org/10.1039/C7RA10237B>
18. Hwang, K.-R., Jeon, W., Lee, S. Y., Kim, M.-S., & Park, Y.-K. (2020). Sustainable bioplastics: Recent progress in the production of bio-building blocks for the bio-based next-generation polymer PEF. *Chemical Engineering Journal*, 390, 124636. <https://doi.org/10.1016/j.cej.2020.124636>
19. Klamt, A. (1995). Conductor-like screening model for real solvents: A new approach to the quantitative calculation of solvation phenomena. *The Journal of Physical Chemistry*, 99, 2224-2235. <https://doi.org/10.1021/j100007a062>
20. Klamt, A. (2005). *COSMO-RS from Quantum Chemistry to Fluid Phase Thermodynamics and Drug Design* (pp.246), Elsevier: Amsterdam, The

- Netherlands.
<https://www.sciencedirect.com/book/9780444519948/cosmo-rs#book-info>
21. Klamt, A., Eckert, F., Reinisch, J., & Wichmann K. (2016). Prediction of cyclohexane-water distribution coefficients with COSMO-RS on the SAMPL5 data set. *Journal of Computer Aided. Molecular Design*, 30, 959-967. <https://doi.org/10.1007/s10822-016-9927-y>
 22. Klamt, A. (2018). The COSMO and COSMO-RS solvation models. *Wiley Interdisciplinary Reviews: Computational Molecular Science*, 1(5), 699-709. <https://doi.org/10.1002/wcms.56>
 23. Kuster, B.F.M. (1990). 5-Hydroxymethylfurfural (HMF). A review focussing on its manufacture. *Starch-Stärke*, 42(8), 314-321. <https://doi.org/10.1002/star.19900420808>
 24. Momany, F., & Schnupf, U. (2014). DFT optimization and DFT-MD studies of glucose, ten explicit water molecules enclosed by an implicit solvent, COSMO. *Computational and Theoretical Chemistry*, 1029, 57-67. <https://doi.org/10.1016/j.comptc.2013.12.007>
 25. Motagamwala, A.H., Huang, K., Maravelias, C.T., & Dumesic, J.A. (2019). Solvent system for effective near-term production of hydroxymethylfurfural (HMF) with potential for long-term process improvement. *Energy & Environmental Science*, 12(7), 2212-2222. <https://doi.org/10.1039/C9EE00447E>
 26. Perlack, R.D., Eaton, L.M., Turhollow Jr, A.F., Langholtz, M.H., Brandt, C.C., Downing, M.E., Graham, R.L., Wright, L.L., Kavkewitz, J.M., & Shamey, A.M. (2011). *US billion-ton update: Biomass supply for a bioenergy and bioproducts industry*. https://www1.eere.energy.gov/bioenergy/pdfs/billion_ton_update.pdf
 27. Rosatella, A.A., Simeonov, S.P., Frade, R.F.M., & Afonso, C.A.M. (2011). 5-Hydroxymethylfurfural (HMF) as a building block platform: Biological properties, synthesis and synthetic applications. *Green Chemistry*, 13(4), 754-793. <https://doi.org/10.1039/C0GC00401D>
 28. Searle, S., & Malins, C. (2015). A reassessment of global bioenergy potential in 2050. *GCB-Bioenergy*, 7(2), 328-336. <https://doi.org/10.1111/gcbb.12141>
 29. Stuart, P.R., & El-Halwagi, M.M. (2012). *Integrated biorefineries: design, analysis, and optimization*. CRC press. <https://www.amazon.com/Integrated-Biorefineries-Optimization-Chemistry-Engineering/dp/1439803463S>
 30. Wang, Z., Bhattacharyya, S., & Vlachos, D.G. (2020). Solvent selection for biphasic extraction of 5-hydroxymethylfurfural via multiscale modeling and experiments. *Green Chemistry*, 22(24), 8699-8712. <https://doi.org/10.1039/D0GC03251D>
 31. Weingarten, R., Rodriguez-Beuerman, A., Cao, F., Luterbacher, J.S., Alonso, D.M., Dumesic, J.A., & Huber, G.W. (2014). Selective conversion of cellulose to hydroxymethylfurfural in polar aprotic solvents. *ChemCatChem*, 6(8), 2229-2234. <https://doi.org/10.1002/cctc.201402299>
 32. Zhang, Y., Guo, X., Tang, P., & Xu, J. (2018). Solubility of 2, 5-furandicarboxylic acid in eight pure solvents and two binary solvent systems at 313.15-363.15 K. *Journal of Chemical & Engineering Data*, 63(5), 1316-1324. <https://doi.org/10.1021/acs.jced.7b00927>
 33. Zhao, X., Farajtabar, A., Han, G., Zhao, H. (2020). Phenformin in aqueous co-solvent mixtures of N, N-dimethylformamide, ethanol, N-methylpyrrolidone and dimethyl sulfoxide: Solubility, solvent effect and preferential solvation. *Journal of Chemical Thermodynamics*, 144, 106085. <https://doi.org/10.1016/j.jct.2020.106085>
 34. Zheng, J., & Suh, S. (2019). Strategies to reduce the global carbon footprint of plastics. *Nature Climate Change*, 9(5), 374-378. <https://www.nature.com/articles/s41558-019-0459-z>
 35. Zunita, M., Wahyuningrum, D., Bundjali, B., Wenten, I.G., & Boopathy, R. (2021). Conversion of glucose to 5-hydroxymethylfurfural, levulinic acid, and formic acid in 1, 3-dibutyl-2-(2-butoxyphenyl)-4, 5-diphenylimidazolium iodide-based ionic liquid. *Applied Sciences*, 11(3), 989. <https://doi.org/10.3390/app11030989>